

Article

Rapid Extreme Tropical Precipitation and Flood Inundation Mapping Framework (RETRACE): Initial Testing for the 2021–2022 Malaysia Flood

Yi Lin Tew ¹, Mou Leong Tan ^{1,*}, Liew Juneng ², Kwok Pan Chun ³, Mohamad Hafiz bin Hassan ⁴, Sazali bin Osman ⁴, Narimah Samat ¹, Chun Kiat Chang ⁵ and Muhammad Humayun Kabir ⁶

- ¹ GeoInformatic Unit, Geography Section, School of Humanities, Universiti Sains Malaysia, Gelugor 11800, Pulau Pinang, Malaysia; tewyilin@student.usm.my (Y.L.T.); narimah@usm.my (N.S.)
 - ² Department of Earth Sciences and Environment, Faculty of Science and Technology, Universiti Kebangsaan Malaysia, Bangi 43600, Selangor, Malaysia; juneng@ukm.edu.my
 - ³ Department of Geography and Environmental Management, University of the West of England, Bristol BS16 1QY, UK; kwok.chun@uwe.ac.uk
 - ⁴ National Flood Forecasting and Warning Centre, Department of Irrigation and Drainage, Kuala Lumpur 68000, Malaysia; hafizhassan@water.gov.my (M.H.b.H.); sazali@water.gov.my (S.b.O.)
 - ⁵ River Engineering and Urban Drainage Research Centre (REDAC), Universiti Sains Malaysia, Engineering Campus, Nibong Tebal 14300, Pulau Pinang, Malaysia; redac10@usm.my
 - ⁶ Department of Agricultural Extension and Information System, Sher-e-Bangla Agricultural University, Dhaka 1207, Bangladesh; dhkahir@sau.edu.bd
- * Correspondence: mouleong@usm.my



Citation: Tew, Y.L.; Tan, M.L.; Juneng, L.; Chun, K.P.; Hassan, M.H.b.; Osman, S.b.; Samat, N.; Chang, C.K.; Kabir, M.H. Rapid Extreme Tropical Precipitation and Flood Inundation Mapping Framework (RETRACE): Initial Testing for the 2021–2022 Malaysia Flood. *ISPRS Int. J. Geo-Inf.* **2022**, *11*, 378. <https://doi.org/10.3390/ijgi11070378>

Academic Editors: Wolfgang Kainz and Godwin Yeboah

Received: 30 April 2022

Accepted: 4 July 2022

Published: 7 July 2022

Publisher's Note: MDPI stays neutral with regard to jurisdictional claims in published maps and institutional affiliations.



Copyright: © 2022 by the authors. Licensee MDPI, Basel, Switzerland. This article is an open access article distributed under the terms and conditions of the Creative Commons Attribution (CC BY) license (<https://creativecommons.org/licenses/by/4.0/>).

Abstract: The 2021–2022 flood is one of the most serious flood events in Malaysian history, with approximately 70,000 victims evacuated daily, 54 killed and total losses up to MYR 6.1 billion. From this devastating event, we realized the lack of extreme precipitation and flood inundation information, which is a common problem in tropical regions. Therefore, we developed a Rapid Extreme TRopicAl preCipitation and flood inundation mapping framEwork (RETRACE) by utilizing: (1) a cloud computing platform, the Google Earth Engine (GEE); (2) open-source satellite images from missions such as Global Precipitation Measurement (GPM), Sentinel-1 SAR and Sentinel-2 optical satellites; and (3) flood victim information. The framework was demonstrated with the 2021–2022 Malaysia flood. The preliminary results were satisfactory with an optimal threshold of five for flood inundation mapping using the Sentinel-1 SAR data, as the accuracy of inundated floods was up to 70%. Extreme daily precipitation of up to 230 mm/day was observed and resulted in an inundated area of 77.43 km² in Peninsular Malaysia. This framework can act as a useful tool for local authorities and scientists to retrace the extreme precipitation and flood information in a relatively short period for flood management and mitigation strategy development.

Keywords: flood; inundation mapping; Sentinel-1 SAR; Malaysia; climate change

1. Introduction

As reported in the Sixth Assessment Report of the Intergovernmental Panel on Climate Change [1], the number and intensity of extreme precipitation has increased significantly in the past few decades. Based on the Emergency Events International Disaster Database [2], a total of 5608 extreme flood events have been recorded around the world from 1906 to 2021, causing about 7 million deaths, affecting 3.9 billion people and causing USD 953 billion in total damage losses. The EM-DAT also reported increases in flood events over the years, particularly in the past two decades. The actual flood losses may be higher as not all flood events were recorded in the EM-DAT database and the costs of damage from floods are difficult to measure. Flood inundation mapping is therefore important to effectively organize flood rescue operations, management, mitigation and modeling to achieve rapid

and effective recovery. In addition, flooded area information could also be used to measure flood damage in cities and agricultural industries.

In Malaysia, major floods are normally found during the early phase of the northeast monsoon (NEM) from November to January; past years of major floods include 1971, 2006–2007, 2014–2015, 2017 and 2018 [3]. Unexpected extreme precipitation events from mid-December 2021 to early 2022 have also caused devastating floods in seven states of Malaysia which killed 54 people, affected more than 125,000 with nearly 70,000 evacuated on a single day and resulted in losses up to MYR 6.1 billion or USD 1.46 billion [4–6]. Surprisingly, the extreme events hit not only the east coast region of Peninsular Malaysia, but also the west coast Peninsular Malaysia that typically experiences dry conditions during this period, where it was noticeable from the direction of the Tropical Depression 29W [7]. Water levels of many rivers and reservoirs in Selangor surpassed their dangerous level. More than 120 landslides occurred a few days after the extreme rains, causing the rescue operations to become more difficult [8]. For instance, the floods and landslides caused the Kuala Lumpur–Karak and the East Coast Expressway phase 1 (LPT1), which connects the east coast and the west coast, to become impassable [9].

The existing flood maps available in Malaysia can be categorized into three types, namely, flood inundation maps, flood hazard maps and flood risk maps [10]. The common practice of producing flood inundation maps in Malaysia involves the coupling of a digital elevation model (DEM) and flood event records [11], or hydrologic and hydraulic simulations performed using tools such as the InfoWorks Integrated Catchment Modeling (ICM) [12]. The production of flood maps via such an approach requires a longer time for data collection, model development and calibration. Despite the importance of near real-time precipitation and flood inundation information, there is still a lack of a comprehensive framework to provide rapid precipitation and flood information during extreme conditions in tropical regions.

Satellite technologies provide a cost-effective and timely resource to capture the precipitation and flood information in a large area during flood events. Satellite precipitation products (SPPs) have emerged as a major source for monitoring global precipitation in the past few decades [13,14]. The Global Precipitation Measurement (GPM) mission, extended from the Tropical Rainfall Measuring Mission (TRMM) [15], is one of the most accurate and finest resolution SPPs to estimate precipitation in tropical regions [16]. The Integrated Multi-Satellite Retrievals for GPM (IMERG) products are able to provide near real-time precipitation data for the regions from 65° N to 65° S at a 30 min time-scale. Tapiador et al. [17] utilized IMERG to study the hydro-meteorological characteristics of the September 2019 floods in Spain and concluded that the IMERG compares well with observations. In China, Qi et al. [18] found the IMERG Late Run (IMERG-Late) product performs well in monitoring the extreme heavy precipitation of the super typhoon Lekima. In Malaysia, Tan and Santo [19] reported that the IMERG products show the lowest bias in capturing precipitation in the 2014–2015 flood events of Malaysia relative to other SPPs. Therefore, the IMERG near real-time products can provide useful information to monitor flood precipitation across the globe.

The European Space Agency's Sentinel-1 Synthetic Aperture Radar (SAR) and Sentinel-2 optical multispectral satellites are becoming popular data sources for effective flood monitoring [20]. Flood mapping using the Sentinel data are mostly conducted in northern temperate latitudes such as Europe, the UK and Canada [21]. In tropical areas, cloud cover is a prevalent issue in optical satellite imagery [22]. Hence, the Sentinel-1 SAR is a preferred satellite sensor for tropical flood monitoring due to it being cloud-free and allowing users to extract time-critical disaster images from the ESA Sentinel Data Hub within 45 min of data capturing [23]. Based on the literature available, the common methodology of analyzing floods via Sentinel-1 data are through classification [24] and thresholding [25]. Thresholding is the most common SAR-based technique for flood detection, but is only perform well in simple flood situations and homogenous land surfaces [26] as it minimalizes classification errors between water and land features without differentiating different land classes [25].

However, identifying an optimal threshold in the binarization and features of elevation differencing takes time and may delay the flood inundation map generation [27], whereby the threshold values are used as the separation value for flood pixels and non-flood pixels in the image [28].

Google Earth Engine (GEE) is a free cloud-based computing platform that enables users to process massive geospatial datasets rapidly using high-performance computing resources [29]. Utilization of GEE in processing Sentinel datasets can achieve rapid flood inundation mapping [26,30]. Therefore, the main aim of this study is to develop a Rapid Extreme TRopical preCipitation and flood inundation mapping framEwork (RETRACE) using the latest satellite technologies, GEE and flood victim information. RETRACE was applied to study the characteristics of the precipitation and floods from the Dec 2021–Jan 2022 unexpected events in Peninsular Malaysia as a pilot study. Three specific objectives of the study are: (1) to investigate the spatio-temporal characteristics of daily precipitation over Peninsular Malaysia using the GPM IMERG product; (2) to identify an optimal threshold for Sentinel-based flood inundation mapping in Malaysia; and (3) to map the inundated flood areas for the 2021–2022 Malaysia flood event. The framework can help local authorities to identify flooded areas, which are vital for flood management and mitigation strategy development. One of the biggest advantages of RETRACE is the capability to provide extreme precipitation and flood inundation information in a relatively shorter period as compared to a traditional flood modeling framework. In addition, the identified optimal threshold for tropical flood inundation mapping and incorporation of flood victim information allows more accurate information to be extracted from satellite images.

2. Materials and Methods

2.1. The 2021–2022 Malaysia Flood

The 2021–2022 flood was among the most serious floods recorded in Malaysia's history, which involved eight states in the Peninsular: Perak, Selangor, Kuala Lumpur, Negeri Sembilan, Melaka, Kelantan, Terengganu and Pahang [31]. Hence, the present study focused on the flooded areas of these largely affected states during the 2021–2022 flood event (Figure 1). Peninsular Malaysia accounts for a majority of Malaysia's population and economy, with a total land area of 132,265 km² and total population of 25.9 million (as of the year 2021) [32].

Situated within the equatorial region, Malaysia has a tropical climate with low atmospheric pressure. The climate of Malaysia is uniform with three major characteristics: constant temperature, high humidity and abundant rainfall throughout the year [33]. The country is situated in a strategic location where it is free from natural catastrophes; however, there are two major hydro-climatic related disasters affecting people's livelihoods: too much rainfall that causes floods and water shortages during the dry period [34]. Among the two hydro-climatic-related disasters, flood is the more devastating natural disaster due to its duration and frequency of occurrence, extent of affected area and the impact it has on the socioeconomic development [35,36].

According to the Department of Irrigation and Drainage (DID) in Malaysia, no formal categorization was made to distinguish floods in Malaysia, but generally floods in Malaysia can be categorized as monsoonal, flash or tidal floods [37], where the differentiation between the monsoonal and flash floods depends on the period of time that the flood water takes to recede. Flash floods are sudden and caused by unpredictable heavy rainfall, whereas monsoonal floods occur during the monsoon seasons [38]. The 2021–2022 flood can be categorized as a monsoonal flood that was caused by the northeast monsoon. In fact, monsoonal floods are a regular annual natural disaster in Malaysia, with major events having occurred in the years of 1926, 1963, 1965, 1967, 1969, 1971, 1973, 1979, 1983, 1993, 1998, 2005, 2006, 2007, 2010, 2014, 2017 and 2021 [38,39]. The northeast monsoonal floods that happened in the past decades in Malaysia are summarized in Table 1.

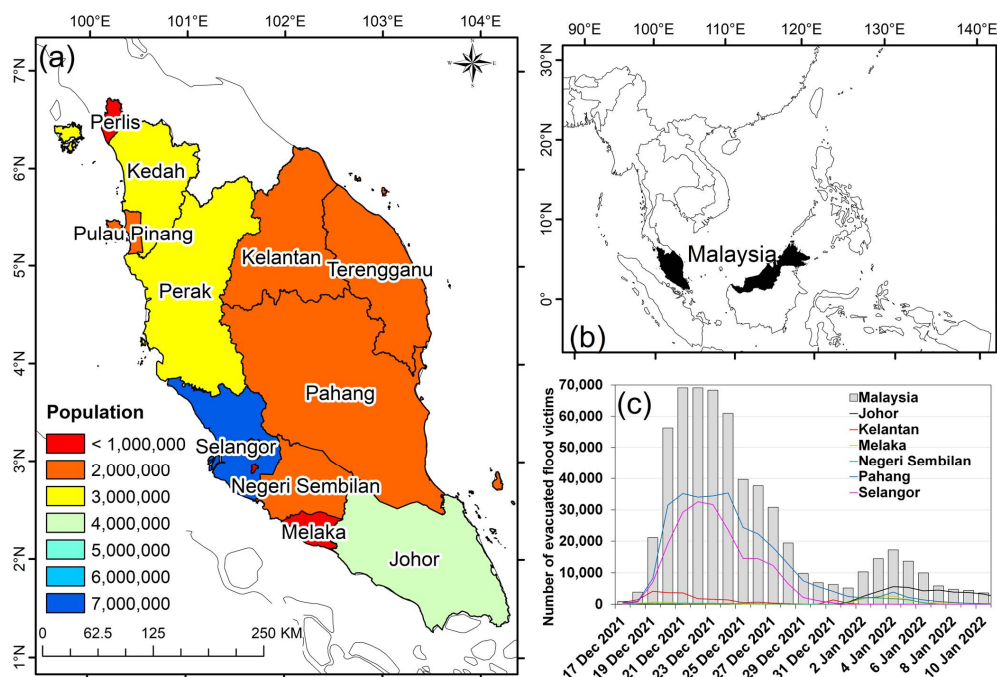


Figure 1. (a) The population for each state in Peninsular Malaysia; (b) location of Malaysia in South East Asia; (c) the number of victims evacuated during the flood event.

Table 1. Description of the floods in Malaysia for the past decade.

Year	Date	States	Outcome	Reference
2010	10 October–19 November	Kedah Perlis	Triggered by a tropical depression and later aggravated by La Nina monsoon rains; 45,000 hectares of rice fields were damaged and government pledged USD 6.5 billion to help the farmers.	
2014	15 December 2014–3 January 2015	Johor Kelantan Kedah Negeri Sembilan Pahang Perak Perlis Sabah Sarawak Selangor Terengganu	Heavy rainfall as part of the northeast monsoon. The worst flood in Kelantan in history with 202,000 individuals evacuated; property damage of USD 560 million.	[36,38–40]
2017	4–5 November	Pulau Pinang	Caused by Tropical Depression 29W on 3 November; flash flood in Pulau Pinang with maximum flood level 3.7 m.	
2021	16–31 December	Perak Selangor Kuala Lumpur Negeri Sembilan Melaka Johor Pahang Terengganu Kelantan Sabah	Caused by Tropical Depression 29W on 14–17 December. Heavy flood in four states and minor flood in four other states; government estimated total of USD 1.55 billion in property damage.	[4,41]

2.2. Global Precipitation Measurement (GPM) Mission

The Global Precipitation Measurement (GPM) mission takes global rainfall and snow-fall observations with a 3 h temporal resolution [16]. The mission was launched by the National Aeronautics and Space Administration (NASA) and the Japan Aerospace Exploration Agency (JAXA) via the Core Observatory (GPM CO) satellite on 28 February 2014, and it was designed as a dual-frequency precipitation radar for precise rainfall measurements. With the sophisticated satellite instrumentation and integrated user applications, the public release of the precipitation product can be acquired in near real-time at 1–5 h post-processing of downlinked observations to ground stations [42].

IMERG is a US GPM Science Team precipitation product that applies intercalibrated estimates over various international constellations of precipitation satellites and conducts monthly surface precipitation gauge analyses to compute higher temporal (half-hourly) and spatial ($0.1^\circ \times 0.1^\circ$) resolutions [43,44]. These characteristics of IMERG precipitation products are advantageous in extreme studies of precipitation globally [21].

2.3. Sentinel Satellites

The Sentinel program is a mission under the European Space Agency [45]. The Sentinel mission operates based on radar and super-spectral imaging for land, ocean and atmospheric monitoring. The data processor includes the Shuttle Radar Topography Mission (SRTM) 1 arc-second data for terrain and radiometric corrections that increases the ease and readiness of Sentinel data for analyzation. The strengths of the data are the ability for it to produce global, continuous and wide-coverage satellite imaging products.

Comprising a constellation of two polar orbiting satellites, the Sentinel-1 mission operates day and night, capturing C-band SAR imagery in all weather. The C-band imaging operating in the Sentinel-1 mission captures the earth with coverage up to 400 km and a spatial resolution of 10 m. The foremost advantage of utilizing the Sentinel-1 SAR data in flood mapping is that the sensor can capture images at wavelengths beyond the cloud cover and thick, moist vegetation cover, regardless if its day- or nighttime [46]. The datasets available in the GEE platform that match with the flood incident in each state for this study are listed in Table 2.

Table 2. The number of available Sentinel datasets in GEE for each state during the 2021–2022 flood in Malaysia.

State	Flood Date	Available Datasets
Pahang	17–31 December	868
Selangor	17–31 December	534
Negeri Sembilan	18–31 December	204
Melaka	17–25 December	199
Johor	05–31 December	708
Terengganu	02–31 December	651
Kelantan	17–31 December	589
Perak	19–21 December	852

The Level-1 Ground Range Detected (GRD) product level data were utilized for water surface detection under the Interferometric Wide Swath (IW) scanning mode, where the phase information was not included. The acquired Sentinel-1 images were $10\text{ m} \times 10\text{ m}$ spatial resolution, with polarization configuration types vertical–horizontal (VH) and vertical–vertical (VV) [47]. The Level-1 GRD products is a package of a dataset that comprises focused SAR data that have been detected, multi-looked and projected to the ground range using the Earth ellipsoid model [23].

Backscattering of the GRD products has been widely used in land cover studies and water body monitoring [48]. Theoretically, VH has a stronger return over areas with volume scattering, whereas VV has a stronger return over specular scattering. Thus, both polarization configurations are used to enhance the band information [49]. SAR images

are often used to map calm and open water surfaces because water surface is recorded as reflected specular incident microwave radiation [50].

2.4. RETRACE

The overall workflow of RETRACE is shown in Figure 2. The Sentinel-1 SAR GRD data were used to generate the flood inundation areas, whereas the Sentinel-2 MSI data were used to collect the ground truth of the flooded area for the purpose of validation. The GPM IMERG Late Run data were used to perform rainfall analysis throughout Peninsular Malaysia during the flood event. The workflow of the processing can be explained in five major steps: (1) pre-processing of the Sentinel-1 and -2 data including subsets of areas of interest, mosaicking, geometric correction, noise removal, etc.; (2) identification of seriously affected areas based on the GPM IMERG precipitation data and flood victim evacuation data; (3) generation of Sentinel-1 SAR flood inundation maps and collection of observed flood data from both sky (Sentinel-2 optical satellite) and ground (site visit); and (4) validation of the flood inundation maps with the observed data. The process was repeated for flood inundation mapping in other affected states.

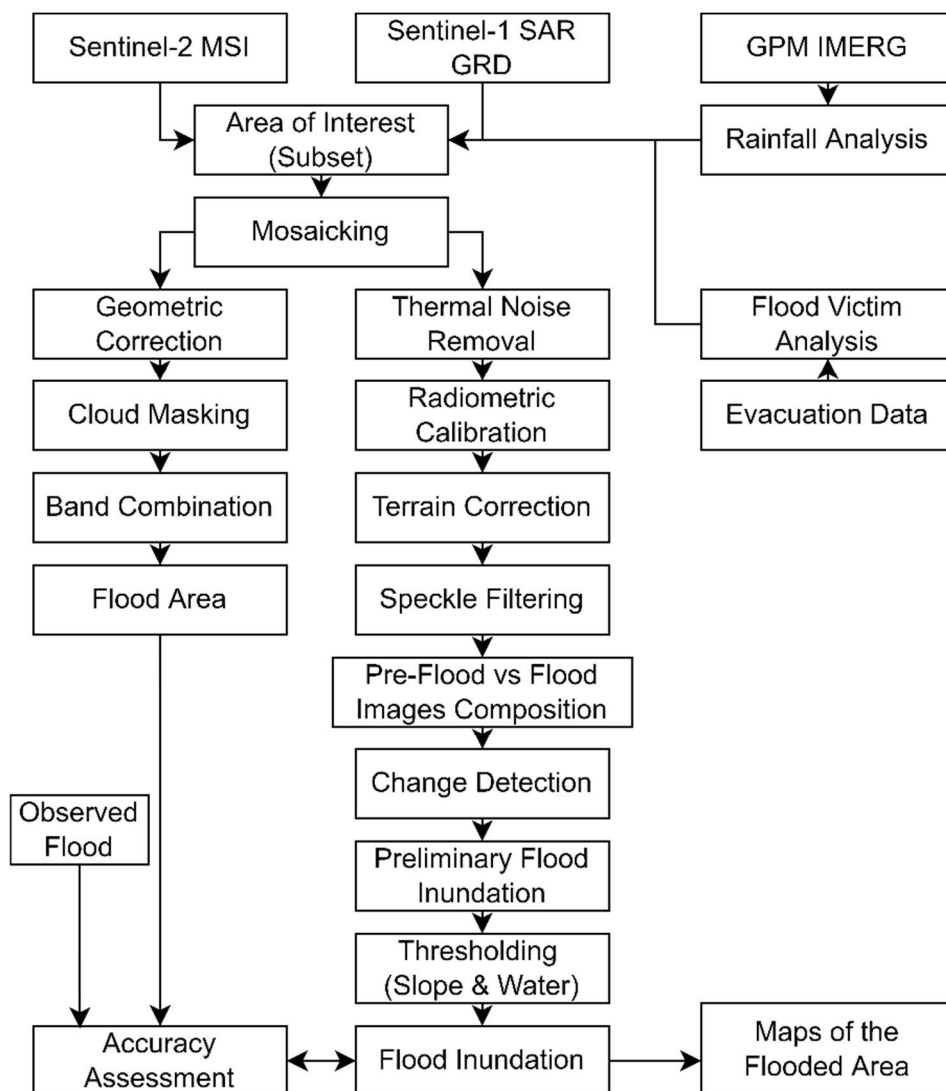


Figure 2. General framework of rapid flood inundation mapping with Sentinel SAR.

The inundation extent of the 2021–2022 Malaysia flood was extracted via an automated thresholding method in the GEE platform, where the results are accessible by the public.

Earth observation satellite data provide a precise and cost-effective tool for assessing and monitoring hydrological dynamics of the earth's surface. As such, multispectral and Synthetic Aperture Radar (SAR) satellite images are advantageous for precipitation monitoring and flood mapping due to their high spatial and temporal resolution characteristics [51]. In the present study, data from two satellites were used to map the flood inundation area throughout the study area: Sentinel-1 SAR images and Sentinel-2 MSI images, where the data are freely accessible via the GEE.

Besides Sentinel data, the Global Administrative Unit Layers 2015 (GAUL), JRC Global Surface Water Mapping Layers, and the WWF HydroSHEDS Void-Filled DEM data in the GEE Data Catalog were also utilized in this study. GAUL is a reliable, global first-level administrative boundary layer made available by the United Nation (UN) Food and Agriculture Organization (FAO) and disseminated based on the 2015 global data [52]. The Global Surface Water Mapping Layers developed by the Joint Research Centre (JRC) of the European Commission (EC) is a global surface water map generated with 4,453,989 Landsat 5, 7, and 8 scenes acquired from 16 March 1984 to 31 December 2020 [53]. Lastly, the HydroSHEDS was developed by the World Wildlife Fund (WWF) and is an elevation hydrographic mapping product at a global scale generated by the Shuttle Radar Topography Mission (SRTM) at a spatial resolution of 3 arc-seconds [54].

2.4.1. Pre-Processing of Sentinel Data

The pre-processing of the Sentinel-1 and -2 datasets included the geometric and radiometric corrections. The Sentinel-1 GRD dataset was retrieved from the GEE platform via instrument mode and received polarization VH, where the date range was set on the driest month of the state for the before-flood period, and the flood dates as stated in Table 1 for the during-flood period.

Then, the dataset was subset with the FAO GAUL data to the extent of each state in Peninsular Malaysia. Radiometric calibration and speckle filtering was conducted at this point, as it is essential to obtain the backscatter values [55]. The radiometrically calibrated images were computed with the radar backscattering coefficient (σ°) associated with SAR image brightness (β°) using the formula:

$$\sigma^\circ = \beta^\circ \cdot \sin \alpha \quad (1)$$

where α is the local incidence angle [28,56]. The return scattering coefficient, σ° , is calculated in decibels [56]:

$$\sigma^\circ(\text{dB}) = 10 \log_{10}(\sigma^\circ) \quad (2)$$

With this, the radar backscattering values can be evaluated using the formula proposed by Laur et al. [56]:

$$\sigma^\circ(\text{dB}) = \beta^\circ(\text{dB}) + 10 \log_{10}[\sin(i_p) / \sin(i_c)] \quad (3)$$

$$\beta^\circ(\text{dB}) = 20 \log_{10}(\text{DN}) - K(\text{dB}) \quad (4)$$

where:

“ i_p ” denotes the pixel's angle of incidence;

“ i_c ” denotes the image center's angle of incidence;

“ K ” denotes the calibration constant of the SAR image.

Then, the smoothing technique was performed to filter out the speckle by eliminating the granular noise that would increase the clarity of the image through application of a speckle filtering window [57]. The process of improving the texture of the SAR image requires computation of Haralick features [58]; thus, we tested different values to observe the dissimilarity. However, the dissimilarity was not presented; thus, the 5×5 window adopted in this study is optimal to optimize the tradeoff between computational time, robustness to outliers and edge preservation [59]. Therefore, the speckle filtering smoothing radius was set at 25 for this study.

2.4.2. Precipitation and Flood Victim Analysis

Basically, IMERG data can be divided into Early Run, Late Run and Final products, which are available ~4 h, ~12 h and ~2 months after capturing the earth surface. The IMERG Late Run product downloaded from the NASA Giovanni online tool (<https://giovanni.gsfc.nasa.gov/giovanni/> (accessed on 11 January 2022)) was used to analyze the spatio-temporal changes of the daily precipitation for Peninsular Malaysia from 15 December 2021 to 7 January 2022. The quality of the IMERG Late Run product is slightly better than the Early Run version due to the calibration scheme in the algorithm; therefore, it is more appropriate for the flood precipitation analysis. This precipitation analysis is conducted to identify the amount of the daily precipitation that has led to the flood in each state of Peninsular Malaysia. IMERG-Late was used to study the spatial and temporal changes of daily precipitation over Malaysia from 17 December 2021 to 10 January 2022 as the explanatory variable to further illustrate the relationship between the climate-induced surface water and flooding extent [60].

The National Disaster Management Agency (NADMA) of Malaysia developed a disaster portal (<https://portalbencana.nadma.gov.my/> (accessed on 11 January 2022)) for reporting the number of flood victims from time to time. At least 89,723 victims were affected daily by the flood in December 2021 [61]. For example, the number of flood victims evacuated from their houses was increased significantly to about 70,000 people per day for three consecutive days since 21 December 2021 (Figure 1c). The second peak of flood victim evacuation was found from 3 to 5 January 2022 due to the second wave of flooding in the state of Johor. The number of flood victims for every state was recorded from the disaster portal from 17 December 2021 to 10 January 2022, and then converted to maps using the ArcMAP 10.4 software.

2.4.3. Flood Inundation Mapping

One of the most efficient and simple approaches for image binarization is through thresholding [62]. In this study, the thresholding was applied via the GEE function that was built from the Otsu's method for image segmentation [63]. Otsu's method is the most widely applied thresholding approach, as it detects the optimum threshold automatically based on the observed distribution of pixel values [64]. In the case of this study, the concept threshold was set in the image processing codes to determine the optimum threshold from the maximization of the between-class variance of the water pixels and the non-water pixels.

The JRC Global Surface Water Mapping Layers was incorporated into the image search result to identify the permanent water areas (sea, rivers and lakes) that exist in the study area which would be classified as flooded surfaces. A threshold of 1.25 was set to extract the Sentinel-1-classified water bodies that, outside the range of the permanent water body, are considered inundated areas, as we were trying to facilitate the detection of flooded surfaces to the pixels with a difference ratio of 0.25 [62]. Then, the WWF HydroSHEDS Void-Filled DEM was utilized to filter the inundation result based on the condition that if the area had a slope larger than 0.5%, it was eliminated from the final inundation result due to the extended nature of the flooded area being mainly flat surfaces.

In flood mapping, the change detection process is performed to analyze the difference between the images for the pre- and post-flood event [62]. As for this study, the processed Sentinel-1 image captured during the flood event was compared with the image captured during the driest month over the region (15–26 February 2021). The pre-flood image was set to obtain any permanent water surfaces over the region, of which this information was later used to mask the overlapping water pixels found on the post-flood image, and the unmasked water pixels were the final inundated extent.

2.4.4. Accuracy Assessment

For the accuracy assessment of the inundation map produced by the Sentinel-1 images, the inundated areas generated by both Sentinel images were cross validated by using the Combine tool in the ArcMap 10.4. This process was conducted for the Pahang and Selangor

states only due to the availability of the cloudless data from the Sentinel-2 sensor during the flood period as shown in Figure 3.

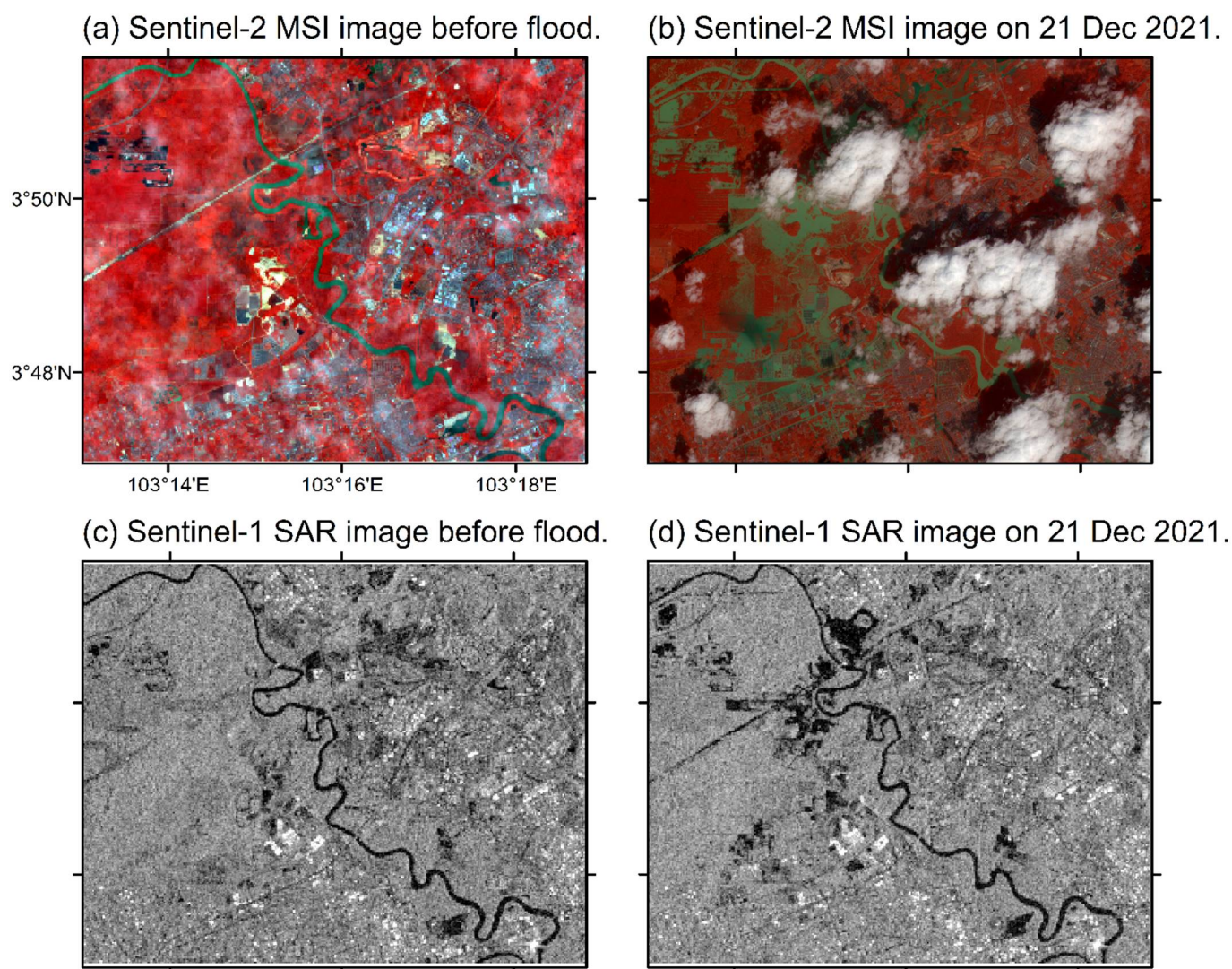


Figure 3. Before- and during-flood satellite images captured by (a,b) Sentinel-2 MSI and (c,d) Sentinel-1 SAR in Kuantan city, Pahang.

The accuracy was assessed on a pixel-by pixel basis for the “flooded” pixel (“0” for non-flooded pixels and “1” for flooded pixels [60]). However, the background class “0” is the majority in a flood mapping and it might cause overestimation in the accuracy of the correctly mapped non-flooded pixels [62]; thus, only the flooded pixels were considered in the accuracy assessment.

As for the validation purposes, the flooded area ground truth points were obtained from the Sentinel-2 MSI data as it was the best-fit dataset available in terms of temporal and spatial resolution during the flood event. Sentinel-2 is a high-spatial-resolution optical sensor under the Global Monitoring for Environment and Security initiative by ESA, where it provides global earth surface information in 13 multispectral bands that cover the visible, near infrared and shortwave infrared range [65].

The Sentinel-2 Level-1B product was used in this study by retrieving the Copernicus Sentinel-2 Surface Reflectance image collection in the GEE platform, where it was radiometric and geometric corrected [66]. The images from 15 to 31 December 2021 were retrieved for a 50% cloud-masked mosaic image over the whole Peninsular Malaysia, where a total of 123 images were composited and mosaicked to form the image scene. The combination

of bands 8 (visible and near infrared), 3 (green) and 2 (blue) was selected to visualize the water content in the image to extract the flooded area.

Unfortunately, due to the limited availability of the Sentinel-2 image during the period, the flooded area points were only managed to be collected for the Pahang and Selangor states. A total of 75 points were collected from the Sentinel-2 image based on the random sampling method on the flooded surfaces. Besides the flood location collected from the Sentinel-2 optical data, we also utilized the observed flood data collected by the National Flood Forecasting and Warning Center (PRABN), DID. The locations where flooding occurred during the 2021–2022 flood event, mostly in the residential areas, were used for the validation purpose. The observed flood data were collected by DID officers on-site when the flood receded. The data provided by PRABN was then filtered to select only the data that had the common record time as the Sentinel images, whereas in this study, a total of 275 matched flood records were adopted for the validation purpose over the Pahang (142 points) and Selangor (133 points) states. Therefore, a total of 350 points (75 points from Sentinel-2 and 275 points from site visits) were used in validating the Sentinel-1 SAR flood inundation maps as shown in Figure 4.

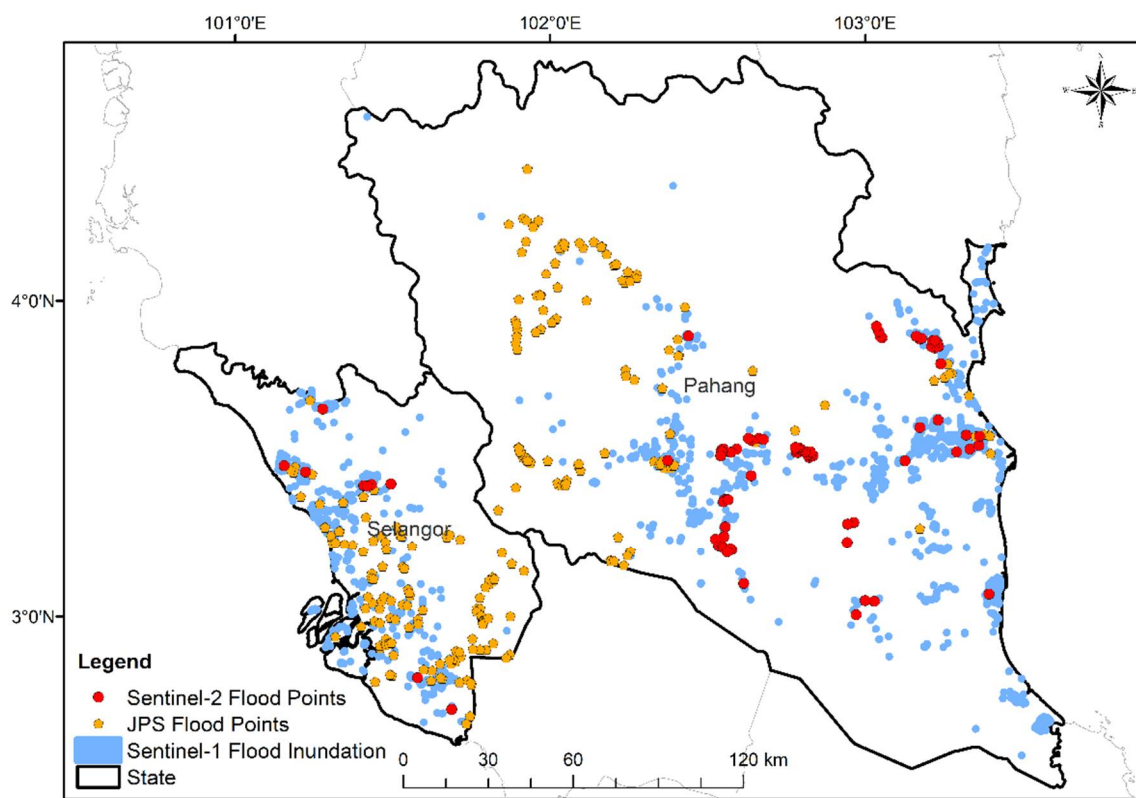


Figure 4. Spatial distribution of the 2021–2022 Malaysia flood events collected from the Sentinel-2 MSI image and observed flood locations.

The critical success index (CSI) was used as the indicator to assess the performance of the flood inundation mapping of the SAR images, as we wanted to assess only the correctly mapped flood pixels rather than the correctly classified non-flooded pixels [62]. The CSI is a suitable performance indicator for comparing the performance of different classification algorithms on the same image rather than classification of flooding between different catchments or a difference of flood magnitudes [67]. The latter is computed as in [68]:

$$CSI = \frac{t_p}{(S_2 + PRABN)} \quad (5)$$

where t_p is the correctly classified flooded pixels, S_2 is the number of flood points collected from the Sentinel-2 image and PRABN is the flood location that was provided by DID.

3. Results

3.1. Flood Victim Analysis

According to the flood victim evacuation reported by NADMA [61], the victims started to be evacuated to the relief centers beginning on 17 December 2021 (Figure 5). The spatial distribution of the evacuated flood victims shows the victims evacuated in Pahang increased drastically from less than 500 on 17 December 2021 to more than 30,000 people on 23 December 2021. Meanwhile, the number of evacuees in Selangor also rose from less than 10,000 people on 19 December 2021 to more than 30,000 people on 23 December 2021 due to the subsiding floods [5]. Based on the flood report, there were a total of 685 temporary relief centers set up across Peninsular Malaysia during the flood event, with the most in Pahang (382 centers). In Malaysia, the flood victim relief centers were managed by the Department of Social Welfare [69]. The relocation of the victims to the relief centers was organized by governmental and non-governmental agencies, based on the conditional analysis performed by the authorities according to the physical factors, i.e., current water level, number of victims for each relief center, and capacity and quantity of the aid and materials that could be supplied.

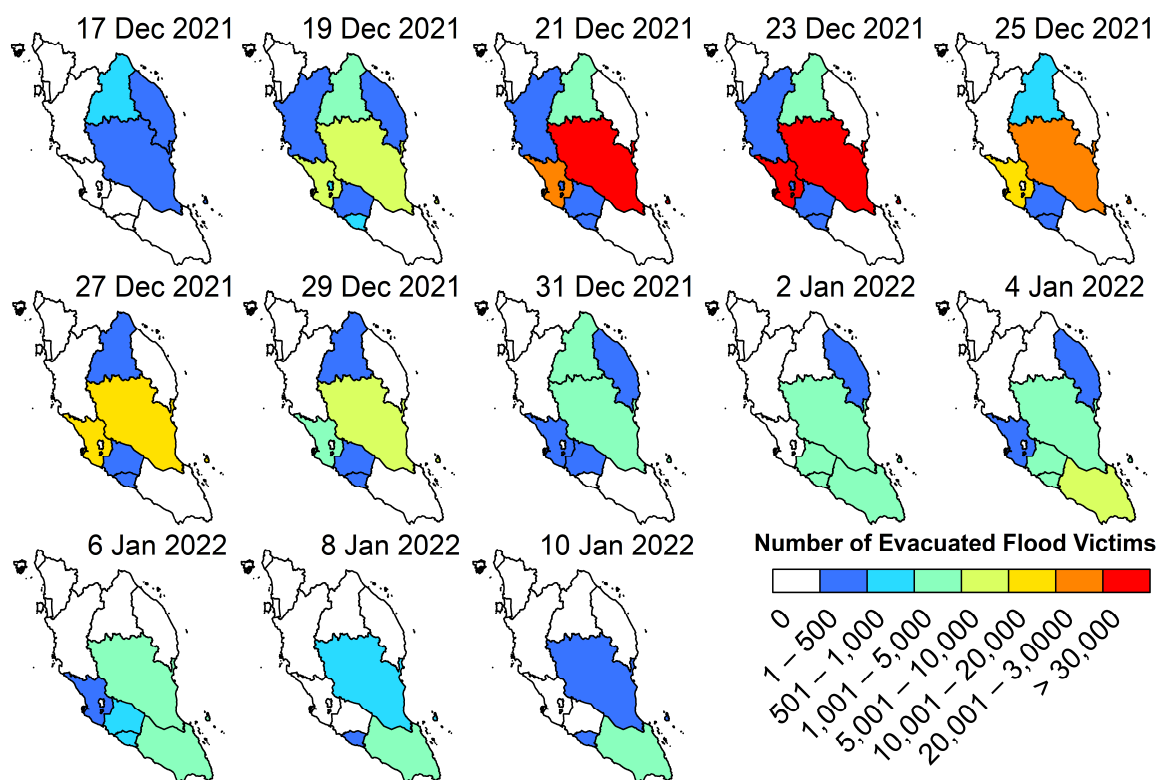


Figure 5. Spatial distribution of evacuated flood victims in Peninsular Malaysia from 19 December 2021 to 10 January 2022.

The statistics of the evacuated flood victims collected were used to validate the reliability of the flood inundation map generated in this study temporally and spatially. The flood victim analysis narrowed the data search of Sentinel-1 and -2 for the generation of the flood inundation extent, as only data from the peak of the flood event day was adopted. Flood victim analysis is an important component in flood management, as it is the first statistic to refer to for analyzing the severity of the flood event spatially [70].

Referring to Figure 5, it can be seen that the flood victims in the Pahang, Terengganu and Kelantan states began to evacuate on 17 December 2021 with less than 500 victims from

each state. The evacuation continued to involve the neighboring states, and Pahang and Selangor reached more than 3000 victims evacuated on 23 December 2021. This information was used for SAR-based flood inundation mapping.

3.2. Extreme Precipitation Analysis

Extreme precipitation is the leading factor of flooding in the tropics [71]. The unexpected extreme precipitation over Peninsular Malaysia from 15 December 2021 to 7 January 2022 was analyzed to identify the number of days and the volume of rainfall across the region (refer to Figures 6 and 7). There was a significant sprout of the precipitation beginning from 16 December 2021 over the states of Pahang, Selangor and Kelantan. Particularly in plot F of Figure 6, it can be seen that daily precipitation in Selangor on the 17 December 2021 was quintuple the amount of the day before. The copious amount of rainfall for these two states continued until 21 December 2021, resulting in an increase in number of victims evacuated. Besides that, more extreme precipitation was observed on 31 December 2021 due to thunderstorms and heavy rain, but there was no flood victim evacuation reported in Selangor since the event was mostly concentrated on the east coast and southern parts of Peninsular Malaysia (Figure 6).

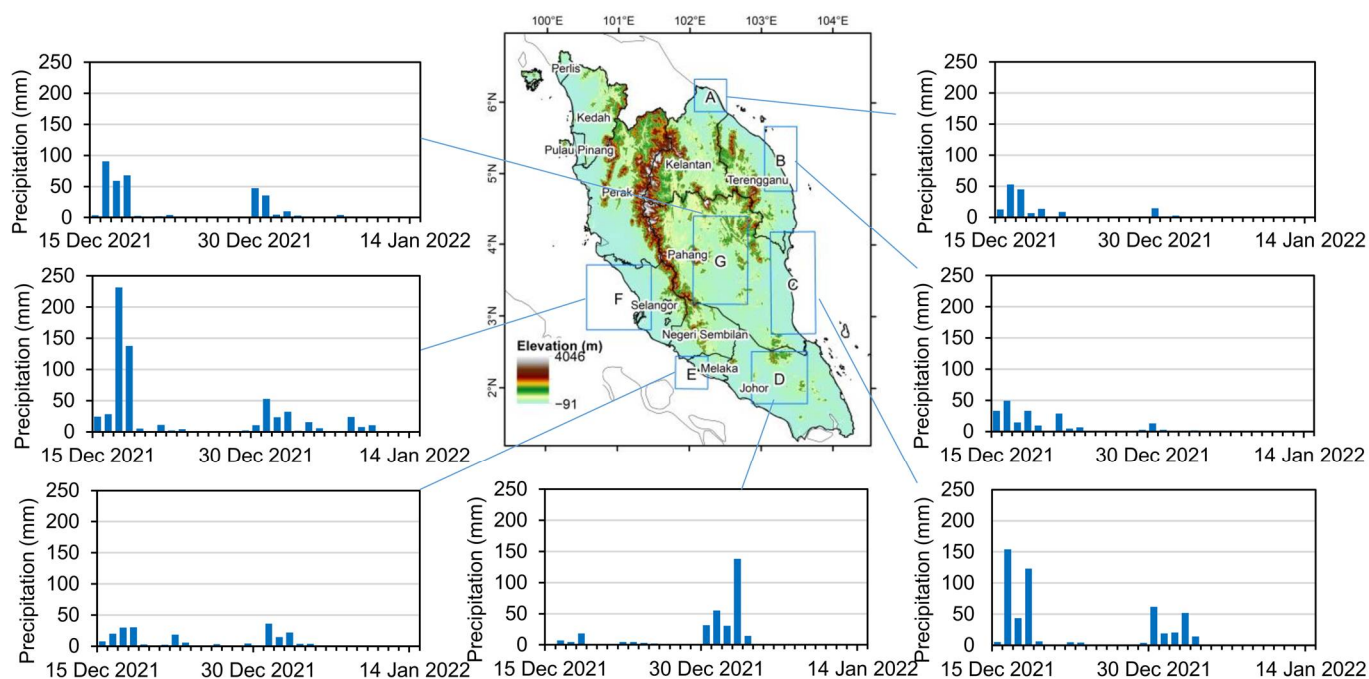


Figure 6. Temporal changes of daily precipitation over Malaysia from 15 December 2021 to 7 January 2022.

The past precipitation trend and precipitation-related extremes on the east coast of Peninsular Malaysia (Pahang, Terengganu and Kelantan) were studied by Mayowa et al. [47] and revealed that there is an increasing trend of the precipitation and precipitation-related extremes in the region over the past 40 years (1971 to 2010). In Pahang (refer to plots C and G), the current study period shows that the intensified precipitation began on 15 December 2021, with the coastal part of Pahang having 50 mm higher daily precipitation (plot C) than the central part of Pahang (plot G). Another notable precipitation sprout in Pahang was on 30 December 2021. This event caused another wave of floods in the state due to the overflowing water levels in the Lipis River and Serting River in central Pahang [72].

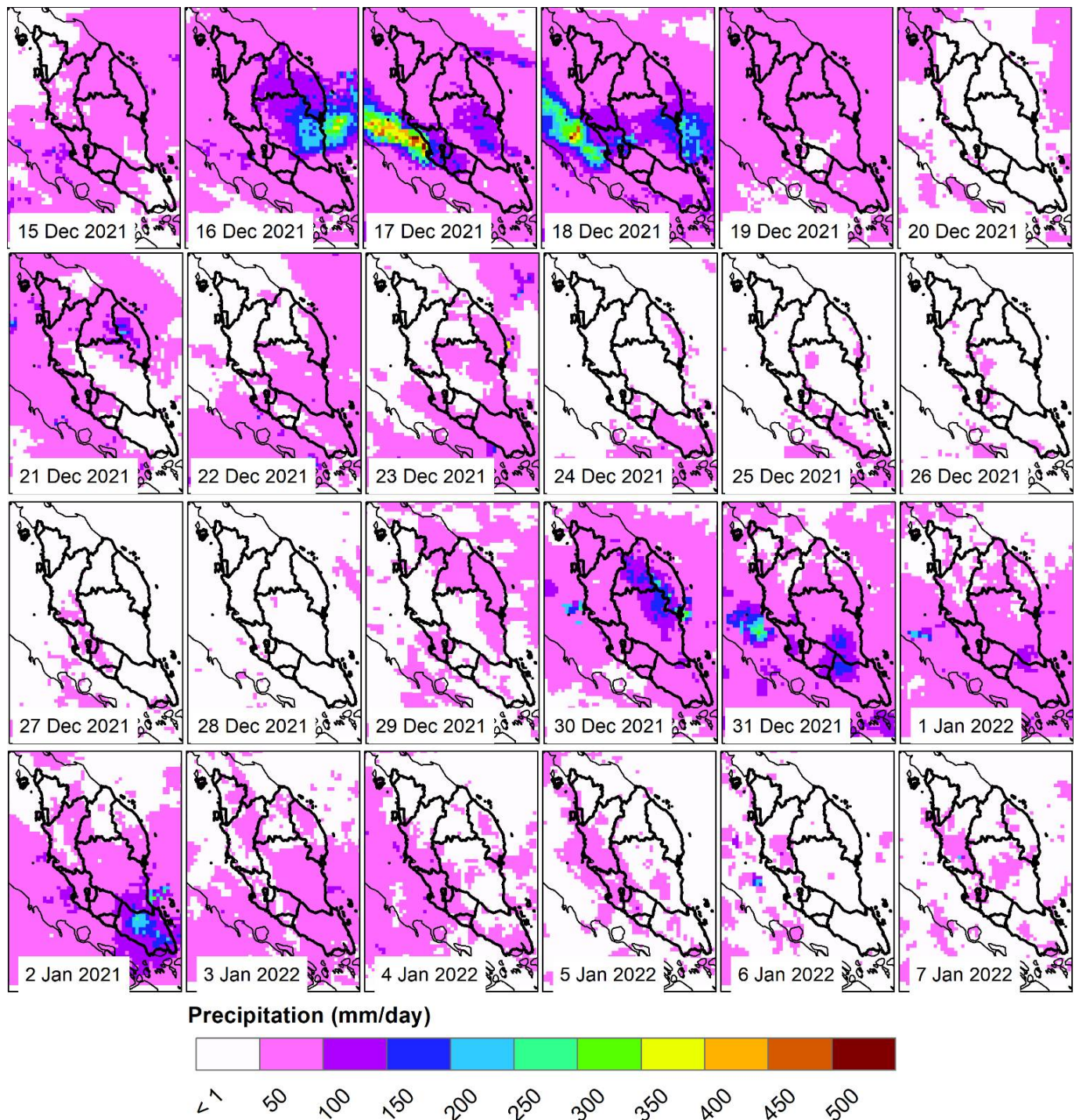


Figure 7. Spatial changes of daily precipitation over Peninsular Malaysia from 17 December 2021 to 10 January 2022.

The above-mentioned second wave of flooding also hit the Johor state (plot D). A precipitation extreme was recorded from 31 December 2021 to 2 January 2022, with daily precipitation above 100 mm. This event caused flooding in northern Johor, leading to the displacement of 1646 victims [73]. However, Johor was the latest state to be affected by the flood, after Negeri Sembilan, Kelantan and Terengganu on the same day [74]. Meanwhile, the precipitation extreme observed on 31 December 2021 for Kelantan (plot A) resulted in 1129 victims being evacuated due to overflowing of the Kelantan River.

Referring to the spatial changes of the daily precipitation in Figure 7 and the evacuation statistics in Figure 4, it is indicated that flood events mostly happened when the precipitation exceeded 100 mm per day. The finding was matched with the study conducted by Tan et al. [13], whereby the extreme flood events in the years of 2006/2007 in the Kelantan, Pahang and Johor states were due to daily precipitation of over 100 mm.

3.3. Accuracy Assessment of Flood Inundation Maps

Due to the availability of cloud-free data from Sentinel-2 images during the flood event, an accuracy assessment was performed only for the Pahang and Selangor states. The accuracy assessment for the inundation mapping of Pahang and Selangor at thresholds of 3-, 4-, and 5-pixel inclusion for distance between the inundated area and the preliminary water surface are shown in Table 3. Both states achieved the best inundation mapping performance when a threshold of 5 was used. Therefore, the same processing approach was adopted for the other states for inundation mapping purposes. The observed flood locations provided by DID were mostly in the residential areas, whereas the flooded areas collected from Sentinel-2 were larger and fall on open spaces and vegetated areas such as rubber estates.

Table 3. Accuracy for each threshold value for Pahang and Selangor states.

Threshold (Pixel)	Pahang (%)	Selangor (%)
3	68.75	61.25
4	69.45	61.88
5	70.20	62.80

3.4. Flood Inundation Mapping for the 2021–2022 Malaysia Flood

The analysis of the Sentinel-1 SAR data shows that the 2021–2022 flood led to the flooding of eight states at a total of 77.435 km². It can be observed that the inundated areas were located downstream of the major rivers, especially in the low-lying areas. Kelantan state had the greatest area flooded (32.32 km²), followed by Pahang (28.87 km²), Johor (8.25 km²) and Selangor (7.24 km²). The total flooded area for each state is tabulated in Table 4 below. Based on the Sentinel-1 SAR-extracted inundated area, the most flooded states during the 2021–2022 Malaysia flood were Pahang (Figure 8), Selangor (Figure 9), Kelantan (Figure 10) and Johor (Figure 11), as compared to the other states with an inundated area of <1 km².

In Pahang state, the inundated area is distributed around the Pahang River, with Pekan district as the most severely flooded district (16.32 km²), followed by Rompin (5.09 km²) and Kuantan (4.21 km²). The extracted inundated area for Temerloh was 0.77 km². The majority of the flooded area in Pahang was residential in low-lying regions that are situated along the riverside. However, although Pahang had the highest number of evacuees, it was not the most flooded state by the total area flooded.

As for Selangor, the most severely flooded district was Kuala Selangor (4.28 km²), where the affected area was mostly residential and industrial. The extracted inundated area for Sabak Bernam was 0.77 km², Kuala Lumpur was 0.014 km², Kuala Langat was 0.95 km² and Ulu Selangor was 0.1 km².

In Kelantan, the inundated area was clustered at the northern part, downstream of the Kelantan River, with Pasir Mas as the most flooded district (11.76 km²). Kota Bharu, the capital city of Kelantan was flooded 11.29 km², followed by Pasir Puteh at 4.4 km², Tumpat at 1.46 km², Machang at 0.73 km² and Tanah Merah at 0.43 km².

Table 4. Flood inundated areas in the selected states of Peninsular Malaysia from December 2021 to January 2022.

State	Flooded Area (km ²)	District	Flooded Area by District (km ²)	Figure		
Pahang (Figure 8a)	28.87	Kuantan	4.21	Figure 8b		
		Temerloh	0.77	Figure 8d		
		Rompin	5.09	Figure 8f		
		Raub	0.02	Figure 8c,e		
		Pekan	16.32			
		Maran	1.14			
		Lipis	0.02			
				Jerantut	0.72	
				Cameron	0.01	
				Bera	0.54	
		Bentong	0.03			
Selangor (Figure 9a)	7.24	Gombak	0.06	Figure 9		
		Klang	0.52	Figure 9c		
		Kuala Selangor	4.28			
		Petaling	0.12	Figure 9b		
		Sabak Bernam	0.77			
		Sepang	0.43			
				Ulu Langat	0.01	Figure 9f Figure 9e
				Ulu Selangor	0.1	
				Kuala Langat	0.95	
Kelantan (Figure 10a)	32.32	Bachok	2.24	Figure 10d		
		Kota Bharu	11.29			
		Kuala Krai	0.01	Figure 10b Figure 10e Figure 10f		
		Pasir Mas	11.76			
		Pasir Puteh	4.4			
				Tanah Merah	0.43	Figure 10c Figure 10f
				Tumpat	1.46	
				Machang	0.73	
Johor (Figure 11a)	8.25	Kota Tinggi	0.54	Figure 11d Figure 11c		
		Batu Pahat	1.6			
		Mersing	0.38	Figure 11b Figure 11f Figure 11e		
		Muar	0.17			
		Pontian	0.44			
				Segamat	2.61	Figure 11b Figure 11f Figure 11e
				Johor Bahru	0.23	
				Kluang	1.5	
				Kulai	0.07	
		Tangkak	0.71			
Kuala Lumpur	0.014					
Melaka	0.63	Jasin	0.27			
		Melaka Tengah	0.1			
		Alor Gajah	0.26			
Negeri Sembilan	0.031	Kuala Pilah	0.005			
		Seremban	0.004			
		Tampin	0.01			
Perak	0.08	Bagan Datuk	0.02			
		Batang Padang	0.01			
		Muallim	0.05			

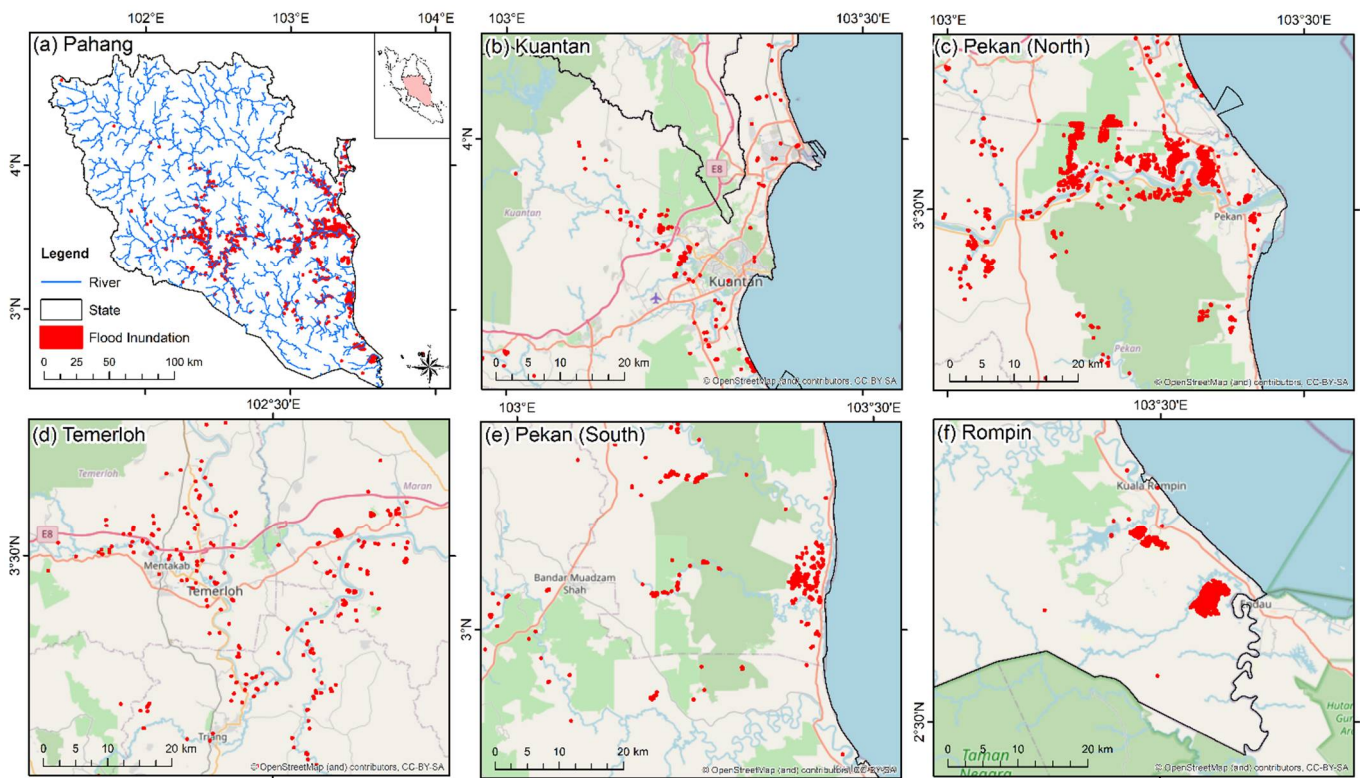


Figure 8. Flood inundation maps of Pahang during the 2021–2022 Malaysia flood.

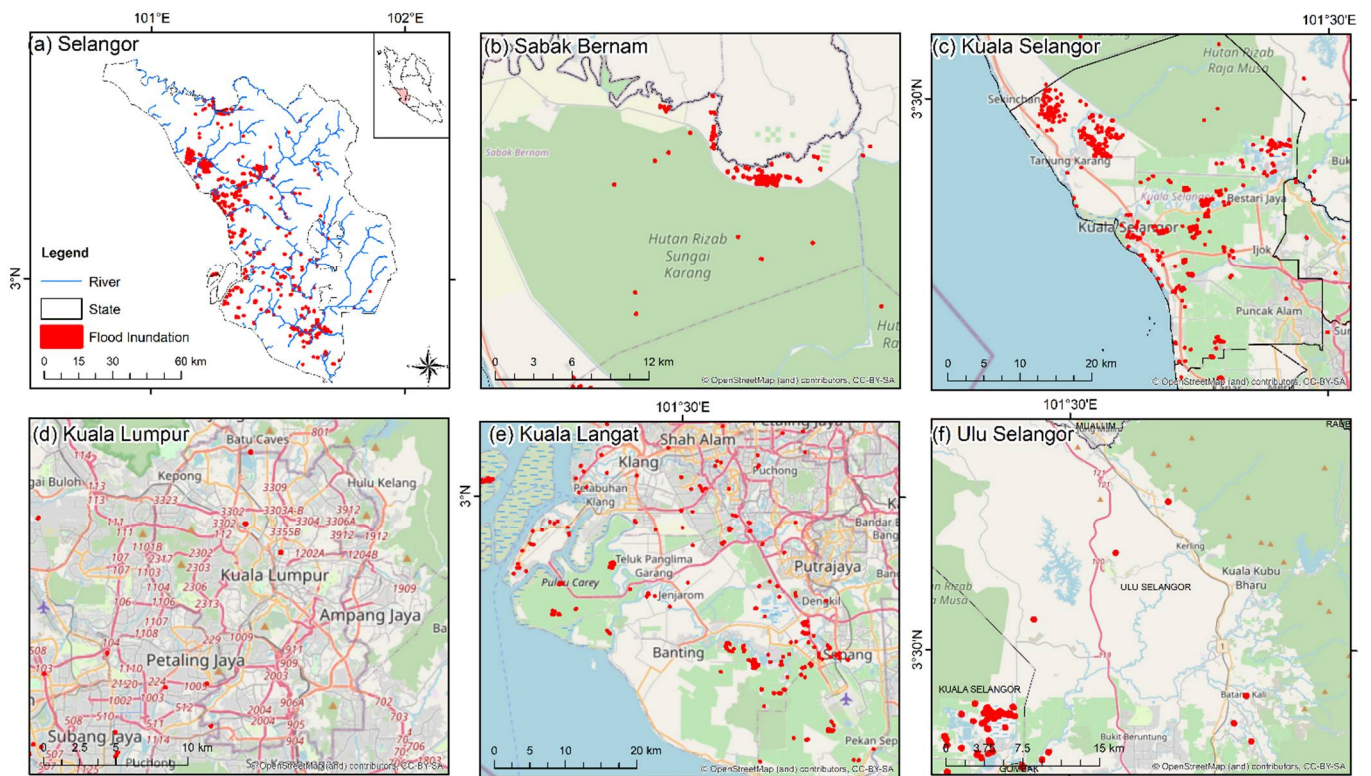


Figure 9. Flood inundation maps of Selangor during the 2021–2022 Malaysia flood.

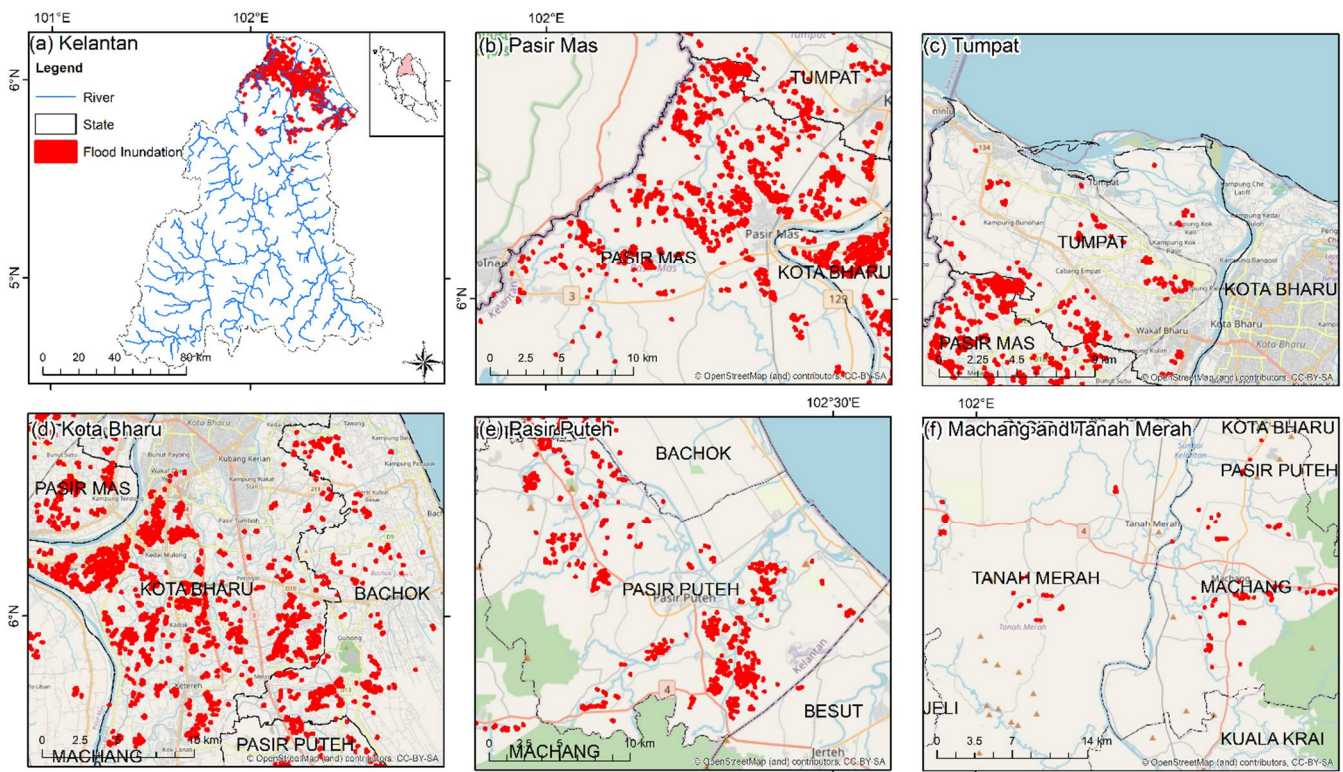


Figure 10. Flood inundation maps of Kelantan during the 2021–2022 Malaysia flood.

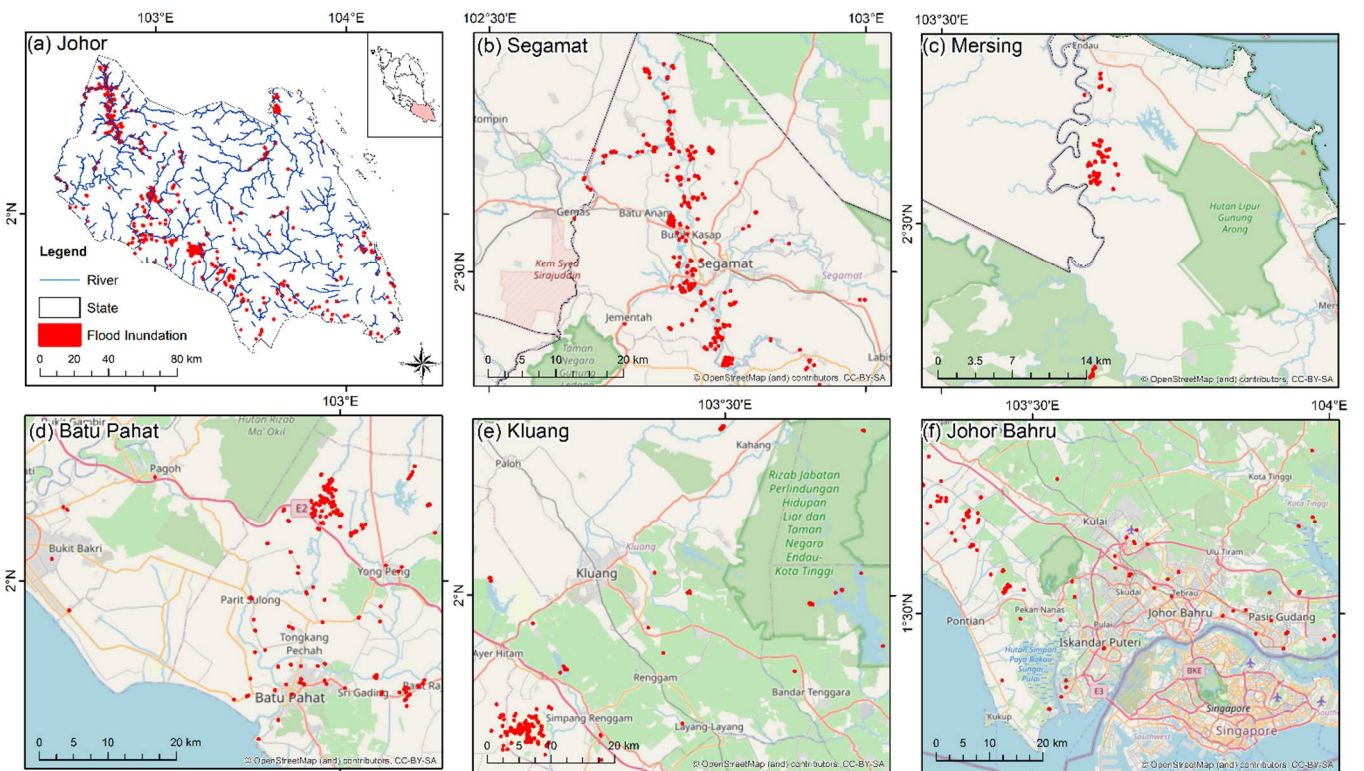


Figure 11. Flood inundation maps of Johor during the 2021–2022 Malaysia flood.

The most inundated district in Johor was Segamat (2.61 km²), which is located in the southern part of Johor. Besides that, Mersing was recorded with flooding of 0.38 km², Batu Pahat had flooding of 1.6 km², Kluang had flooding of 1.5 km², and Johor Bahru, the capital city of Johor, was flooded 0.23 km².

4. Discussion

4.1. GPM Precipitation Analysis

GPM IMERG products have been applied to study flash floods and monsoonal floods around the world. Based on the precipitation changes observed by the GPM satellites, extremely heavy daily precipitation of up to 230 mm/day was recorded over Selangor from 17 to 19 December 2021 (Figure 5). Please note that the GPM IMERG near real-time products tended to underestimate daily precipitation in Malaysia during the 2014–2015 flood by 3.09 to 24.19% [19]. Therefore, the actual precipitation amount that reached the ground surface during the 2021–2022 flood may be higher than the ones observed by the GPM IMERG Late Run product. A comprehensive validation of the GPM IMERG and other satellite precipitation products in capturing the extreme precipitation (up to hourly assessment) during flood periods over Malaysia should be conducted in the future.

Meanwhile, the precipitation analysis for the 2021–2022 Malaysia flood event is consistent with the results reported by Mayowa et al. [72] and Liang et al. [75], in which an extreme flood event happens in the east coast part of Peninsular Malaysia when the daily precipitation exceeds 100 mm per day. Extreme precipitation and flood events have increased significantly in terms of frequency and intensity in tropical regions. Hence, proper mitigations and strategies for flood management need to be made to deal with the increasing trend of extreme flood events in Malaysia [76], and flood inundation maps produced from Sentinel-1 SAR could be an extremely useful source for comparing with the flood modeling outputs.

4.2. The 2021–2022 Malaysia Flood

During the past flood events, the Mineral and Geoscience Department reported a total of 121 landslides occurred nationwide, following the yellow alert for continuous rain by the Malaysian Meteorological Department [4]. The topography of Peninsular Malaysia is hilly in the central spine and flat towards the coastal lines, where landslides that happen along the Pahang and Langat Rivers are believed to contribute to the cause of the flood event [8]. The landslides carried debris and formed debris streams across several major rivers in Peninsular Malaysia and, thus, led to the flood. In this study, we identified the extent and total area flooded for each state through analyzing Sentinel-1 SAR images. The results showed the flooded areas were mostly saturated along the major river, whereby the areas were lower in terms of elevation. Kelantan had the largest area flooded among the other states, whereas Pahang had the greatest number of victims evacuated during the flood.

The idea of mapping flood inundation with SAR images can solve the challenges of producing real-time flood extent information when it is hard to access the flooded area. In fact, many tropical countries do not own remote sensing satellites that allow them to fully operate or control the satellite for monitoring disasters in their own land. This study can provide useful references for the authorities and decision makers in Malaysia for future flood hazard management with remote sensing technologies. The ability of SAR images to capture real-time flood areas at a large scale adds value in flood mapping, especially for remote areas [57]. Sentinel-1 SAR is a free and open-source SAR dataset for various applications on the GEE platform and is beneficial for the public to assess geographical issues.

4.3. Limitations of the Study

Nevertheless, there are a few limitations of this study that should be addressed in the future with better solutions, especially in terms of data availability and processing

considerations. Sentinel-1 SAR has a revisit time of 6–12 days on average, where in some cases we were not able to obtain the data exactly on the day when flooding hit the area. Thus, alternatively in this study, we stacked a period of five days before the flood and five days after the flood to obtain a differencing image that showed the flooded area. However, this might not be a practical method for precise inundation mapping as the real-time flood situation was not captured. The same issue applies for Sentinel-2 MSI data, and the flood region estimated on Sentinel-2 images might be overestimated as clouds are intense during flood events [77]. In addition, based on the analysis of the inundated area results, we found that the flood in the built-up area might not be as complete as what we expected. This might be due to finer information lost during the speckle filtering or elevation delineation.

This work may be improved in the future by considering more polarization [78] or data fusion, as suggested by Tulbure et al. [60]. They demonstrated the improvement of flood mapping via fusion of different datasets, but the study found that mapping of open water surfaces in terms of flooding is still challenging as the spectral signatures may be affected by sediment load, turbidity, dissolved matters, algae content depth and a bottom reflectance signal [79]. Mason et al. [68] suggested that merging very high-resolution SAR digital slope model (DSM) data could map urban flooding more accurately.

5. Conclusions

The 2021–2022 flood was the most deliberate flood in Malaysia's history in terms of property damage; however, a lack of flood inundation information resulted in difficulties in rescue planning and resource management during and after the flood event. Hence, this study developed a Rapid Extreme TRopicAl preCipitation and flood inundation mapping framEwork (RETRACE) for helping local authorities with flood planning and mitigation strategy development. Open-source satellite images from missions such as the GPM IMERG Late Run product for precipitation and Sentinel-1 SAR for flood inundation mapping were fully utilized in this framework. The flood victim statistics, which can be obtained from NADMA and/or social media, are important inputs for any flood-related studies. In addition, most of the processes were conducted using the cloud computing system, Google Earth Engine (GEE), to save processing time and cost. This framework was applied to study the characteristics of precipitation and floods for the Dec 2021–Jan 2022 unexpected precipitation events in Peninsular Malaysia.

Overall, two peaks in the number of flood victims evacuated from their houses were observed: (1) 21–24 December 2021—60,000 to 70,000 flood victims were placed in relief centers, mostly in Pahang and Selangor; and (2) 2–6 January 2022—10,000 to 15,000 people relocated to relief centers in Johor. Intense daily rainfall of up to 230 mm/day over Peninsular Malaysia during the period triggered extreme flooding in eight states, primarily in Pahang, Selangor, Kelantan and Johor. This analysis is important for future hazard management so that an early warning can be released when the forecasted rainfall exceeds the danger volume, as well as establishing preparations for flood relief operations during monsoon seasons.

Sentinel-1 SAR images were able to produce flood inundation maps for the 2021–2022 flood. The result was validated with the flood location extracted from Sentinel-2 MSI images and observed floods collected from site visits. The total flooded area in Peninsular Malaysia during the flood was 77.43 km², and the spatial distribution of the inundated area shows that the flood was saturated along the major rivers. The result shows that the presented framework could produce flood inundated maps at 62~70% accuracy with the threshold values suggested in this study. The maps are useful for local authorities such as DID for use in flood management and to compare with the flooded areas simulated using flood models.

Author Contributions: Conceptualization, Mou Leong Tan, Yi Lin Tew and Liew Juneng; methodology, Mou Leong Tan and Yi Lin Tew; validation, Yi Lin Tew, Mohamad Hafiz bin Hassan and Sazali bin Osman; formal analysis, Mou Leong Tan, Yi Lin Tew and Kwok Pan Chun; resources, Mou Leong Tan and Narimah Samat; writing—original draft preparation, Yi Lin Tew and Mou Leong Tan; writing—review and editing, Mou Leong Tan, Liew Juneng, Kwok Pan Chun, Chun Kiat Chang and Muhammad Humayun Kabir; supervision, Mou Leong Tan and Narimah Samat; funding acquisition, Mou Leong Tan and Narimah Samat. All authors have read and agreed to the published version of the manuscript.

Funding: This research was funded by the Ministry of Higher Education Malaysia under the Long-Term Research Grant Scheme Project 2, grant number LRGS/1/2020/UKM-USM/01/6/2, which is under the program of LRGS/1/2020/UKM/01/6.

Institutional Review Board Statement: Not applicable.

Informed Consent Statement: Not applicable.

Data Availability Statement: Sentinel data presented in this study are available in Google Earth Engine (<https://earthengine.google.com/> (accessed on 11 January 2022)). The IMERG Late Run product is available from the NASA Giovanni online tool (<https://giovanni.gsfc.nasa.gov/giovanni/> (accessed on 11 January 2022)). Observed flood data are available on request from DID Malaysia. The code of flood inundation mapping is available at <https://code.earthengine.google.com/?scriptPath=users%2Ftewyilin%2FPublic%3ARETRACE> (accessed on 6 July 2022).

Acknowledgments: The authors would like to express gratitude to the developers of GEE, GPM, and Sentinel for providing free satellite data and cloud computing platforms to the public. The authors also thank DID and NADMA for providing the observed flood and flood victim information. K P Chun is the awardee of the Accelerator Programme (AP) 2022-24 in the University of the West of England (UWE), Bristol. The authors also acknowledge the editors and reviewers for their valuable suggestions to improve this manuscript.

Conflicts of Interest: The authors declare no conflict of interest.

References

1. IPCC. AR6 Climate Change 2021: The Physical Science Basis. In *Working Group 1*; Cambridge University Press: Cambridge, UK; New York, NY, USA, 2021; p. 1300.
2. EM-DAT. EM-DAT: The Emergency Events Database. 2022. Available online: www.emdat.be (accessed on 1 April 2022).
3. Tang, Z.; Li, Y.; Gu, Y.; Jiang, W.; Xue, Y.; Hu, Q.; LaGrange, T.; Bishop, A.; Drahota, J.; Li, R. Assessing Nebraska playa wetland inundation status during 1985–2015 using Landsat data and Google Earth Engine. *Environ. Monit. Assess.* **2016**, *188*, 1–14. [[CrossRef](#)] [[PubMed](#)]
4. Bernama. *Floods: 10 Missing in Pahang, Selangor Worst Hit State*; Astro Awani: Kuala Lumpur, Malaysia, 2021.
5. Bernama. *Flood Situation Worsens as at Afternoon, More Than 34,000 Victims Evacuated*; The Sun Daily: Kuala Lumpur, Malaysia, 2021.
6. Reuters. *Floods Hit Seven States in Malaysia, Thousands More Evacuated, in Reuters*; Reuters: Kuala Lumpur, Malaysia, 2022.
7. Rahman, S. *Malaysia's Floods of December 2021: Can Future Disasters be Avoided? Researchers at ISEAS–Yusof Ishak Institute Analyse Current Events*; ISEAS–Yusof Ishak Institute: Singapore, 2022.
8. Ong, H.S. *Expert: Debris Flood in Pahang and Selangor Caused by Multiple Landslides, Streams of Waste*; The Star: Kuantan, Malaysia, 2022.
9. NATION. *Flood Alert: Sections of KL–Karak Highway Impassable Due to Water, landslides*; The Star: Kuantan, Malaysia, 2021.
10. Zakaria, S.F.; Mohamad Zin, R.; Mohamad, I.; Balubaid, S.; Mydin, S.H.; MDR, E.R. The Development of Flood Map in Malaysia. *AIP Conf. Proc.* **2017**, *1903*, 110006.
11. Ab Ghani, A.; Chang, C.K.; Leow, C.S.; Zakaria, N.A. Sungai Pahang digital flood mapping: 2007 flood. *Int. J. River Basin Manag.* **2012**, *10*, 139–148. [[CrossRef](#)]
12. Liew, Y.S.; Mat Desa, S.; Noh, M.N.M.; Tan, M.L.; Zakaria, N.A.; Chang, C.K. Assessing the Effectiveness of Mitigation Strategies for Flood Risk Reduction in the Segamat River Basin, Malaysia. *Sustainability* **2021**, *13*, 3286. [[CrossRef](#)]
13. Tan, M.L.; Ibrahim, A.L.; Duan, Z.; Cracknell, A.P.; Chaplot, V. Evaluation of Six High-Resolution Satellite and Ground-Based Precipitation Products over Malaysia. *Remote Sens.* **2015**, *7*, 1504–1528. [[CrossRef](#)]
14. Tan, M.L.; Gassman, P.W.; Liang, J.; Haywood, J.M. A review of alternative climate products for SWAT modelling: Sources, assessment and future directions. *Sci. Total Environ.* **2021**, *795*, 148915. [[CrossRef](#)]
15. Huffman, G.J.; Bolvin, D.T.; Nelkin, E.J.; Wolff, D.B.; Adler, R.F.; Gu, G.; Hong, Y.; Bowman, K.P.; Stocker, E.F. The TRMM Multisatellite Precipitation Analysis (TMPA): Quasi-Global, Multiyear, Combined-Sensor Precipitation Estimates at Fine Scales. *J. Hydrol.* **2007**, *8*, 38–55. [[CrossRef](#)]

16. Hou, A.Y.; Kakar, R.K.; Neeck, S.; Azarbarzin, A.A.; Kummerow, C.D.; Kojima, M.; Oki, R.; Nakamura, K.; Iguchi, T. The Global Precipitation Measurement Mission. *Bull. Am. Meteorol. Soc.* **2014**, *95*, 701–722. [[CrossRef](#)]
17. Tapiador, F.J.; Marcos, C.; Sancho, J.M.; Santos, C.; Núñezb, J.Á.; Navarroc, A.; Kummerowd, C.; Adlere, R.F. The September 2019 floods in Spain: An example of the utility of satellite data for the analysis of extreme hydrometeorological events. *Atmos. Res.* **2021**, *257*, 105588. [[CrossRef](#)]
18. Qi, W.; Yong, B.; Gourley, J.J. Monitoring the super typhoon lekima by GPM-based near-real-time satellite precipitation estimates. *J. Hydrol.* **2021**, *603*, 126968. [[CrossRef](#)]
19. Tan, M.L.; Santo, H. Comparison of GPM IMERG, TMPA 3B42 and PERSIANN-CDR satellite precipitation products over Malaysia. *Atmos. Res.* **2018**, *202*, 63–76. [[CrossRef](#)]
20. Kuntla, S.K. An era of Sentinels in flood management: Potential of Sentinel-1, -2, and -3 satellites for effective flood management. *Open Geosci.* **2021**, *13*, 1616–1642. [[CrossRef](#)]
21. Zhang, D.; Yang, M.; Ma, M.; Tang, G.; Wang, T.; Zhao, X.; Ma, S.; Wu, J.; Wang, W. Can GPM IMERG Capture Extreme Precipitation in North China Plain? *Remote Sens.* **2022**, *14*, 928. [[CrossRef](#)]
22. Li, Z.; Shen, H.; Cheng, Q.; Li, W.; Zhang, L. Thick Cloud Removal in High-Resolution Satellite Images Using Stepwise Radiometric Adjustment and Residual Correction. *Remote Sens.* **2019**, *11*, 1925. [[CrossRef](#)]
23. Twele, A.; Cao, W.; Plank, S.; Martinis, S. Sentinel-1-based flood mapping: A fully automated processing chain. *Int. J. Remote Sens.* **2016**, *37*, 2990–3004. [[CrossRef](#)]
24. Huang, W.; DeVries, B.; Huang, C.; Lang, M.W.; Jones, J.W.; Creed, I.F.; Carroll, M.L. Automated Extraction of Surface Water Extent from Sentinel-1 Data. *Remote Sens.* **2018**, *10*, 797. [[CrossRef](#)]
25. Liang, J.; Liu, D. A local thresholding approach to flood water delineation using Sentinel-1 SAR imagery. *ISPRS J. Photogramm. Remote Sens.* **2019**, *159*, 53–62. [[CrossRef](#)]
26. Zhang, M.; Chen, F.; Liang, D.; Tian, B.; Yang, A. Use of Sentinel-1 GRD SAR Images to Delineate Flood Extent in Pakistan. *Sustainability* **2020**, *12*, 5784. [[CrossRef](#)]
27. Manjusree, P.; Kumar, L.P.; Bhatt, C.M.; Rao, G.S.; Bhanumurthy, V. Optimization of threshold ranges for rapid flood inundation mapping by evaluating backscatter profiles of high incidence angle SAR images. *Int. J. Disaster Risk Sci.* **2012**, *3*, 113–122. [[CrossRef](#)]
28. Tripathi, G.; Pandey, A.C.; Parida, B.R.; Kumar, A. Flood Inundation Mapping and Impact Assessment Using Multi-Temporal Optical and SAR Satellite Data: A Case Study of 2017 Flood in Darbhanga District, Bihar, India. *Water Resour. Manag.* **2020**, *34*, 1871–1892. [[CrossRef](#)]
29. Gorelick, N.; Hancher, M.; Dixon, M.; Ilyushchenko, S.; Thau, D.; Moore, R. Google Earth Engine: Planetary-scale geospatial analysis for everyone. *Remote Sens. Environ.* **2017**, *202*, 18–27. [[CrossRef](#)]
30. Uddin, K.; Matin, M.A.; Meyer, F.J. Operational Flood Mapping Using Multi-Temporal Sentinel-1 SAR Images: A Case Study from Bangladesh. *Remote Sens.* **2019**, *11*, 1581. [[CrossRef](#)]
31. AHA. *Flooding in 8 States Malaysia—Flash Update #1*; AHA Center: Jakarta Timur, Indonesia, 2021.
32. DOSM. Launching of Report on the Key Findings Population and Housing Census Of Malaysia 2020. Brief Report on Key Findings Population and Housing Census of Malaysia 2020. Available online: https://www.dosm.gov.my/v1/index.php?r=column/cthemeb-Cat&cat=117&bul_id=akliVWdIa2g3Y2VubTVSMkxmYXp1UT09&menu_id=L0pheU43NWJwRWVVSZklWdzQ4TlhUUT09 (accessed on 3 March 2022).
33. Tan, M.L.; Juneng, L.; Tangang, F.T.; Chunag, J.X.; Radin Firdaus, R.B. Changes in Temperature Extremes and Their Relationship with ENSO in Malaysia from 1985 to 2018. *Int. J. Climatol.* **2020**, *41*, E2564–E2580. [[CrossRef](#)]
34. Tang, K.H.D. Climate change in Malaysia: Trends, contributors, impacts, mitigation and adaptations. *Sci. Total Environ.* **2018**, *650*, 1858–1871. [[CrossRef](#)]
35. Ismail, M.S.N.; Abdul Ghani, A.N.; Md Ghazaly, Z. The characteristics of road inundation during flooding events in Peninsular Malaysia. *Int. J. GEOMATE* **2019**, *54*, 129–133.
36. Mohd Taib, Z.; Jaharuddin, N.S.; Mansor, Z. A Review of Flood Disaster and Disaster Management in Malaysia. *Int. J. Account. Bus. Manag.* **2016**, *4*, 9.
37. DID. Flood Management-Programme and Activities. 2017. Available online: <https://www.water.gov.my/index.php/pages/view/419> (accessed on 3 March 2022).
38. Shah, S.M.H.; Mustafa, Z.; Yusof, K.W. Disasters Worldwide and Floods in the Malaysian Region: A Brief Review. *Indian J. Sci. Technol.* **2017**, *10*, 9. [[CrossRef](#)]
39. Ibrahim, N.A.; Wan Alwi, S.R.; Abdul Manan, Z.; Mustafa, A.A.; Kidam, K. Flood Impact on Renewable Energy System in Malaysia. *Chem. Eng. Trans.* **2021**, *89*, 193–198.
40. Durumin Iya, S.G.; BarzaniGasim, M.; EkhwanToriman, M.; Abdullahi, M.G. Floods in Malaysia: Historical Reviews, Causes, Effects and Mitigations Approach. *Int. J. Interdiscip. Res. Innov.* **2014**, *2*, 50–65.
41. Aiman, A. *Flood Losses 'Could Amount to RM20 Billion'*; Free Malaysia Today: Petaling Jaya, Malaysia, 2021.
42. Skofronick-Jackson, G.; Petersen, W.A.; Berg, W.; Kidd, C.; Stocker, E.F.; Kirschbaum, D.B.; Kakar, R.; Braun, S.A.; Huffman, G.J.; Iguchi, T.; et al. The Global Precipitation Measurement (GPM) Mission for Science and Society. *Bull. Am. Meteorol. Soc.* **2017**, *98*, 1679–1695. [[CrossRef](#)]

43. Huffman, G.J.; Bolvin, D.T.; Braithwaite, D.; Hsu, K.-L.; Joyce, R.J.; Kidd, C.; Nelkin, E.J.; Sorooshian, S.; Stocker, E.F.; Tan, J. Integrated multi-satellite retrievals for the Global Precipitation Measurement (GPM) mission (IMERG). In *Satellite Precipitation Measurement*; Springer: Cham, Switzerland, 2020; pp. 343–353.
44. Pradhan, R.K.; Markonis, Y.; Godoy, M.R.V.; Villalba-Pradas, A.; Andreadis, K.M.; Nikolopoulos, E.I.; Papalexiou, S.M.; Rahim, A.; Tapiador, F.J.; Hanel, M. Review of GPM IMERG performance: A global perspective. *Remote Sens. Environ.* **2021**, *268*, 112754. [[CrossRef](#)]
45. ESA. The Sentinel Missions. 2022. Available online: https://www.esa.int/Applications/Observing_the_Earth/Copernicus/The_Sentinel_missions#:~:text=ESA%20is%20developing%20a%20new,robust%20datasets%20for%20Copernicus%20services (accessed on 2 March 2022).
46. Potin, P.; Bargellini, P.; Laur, H.; Rosich, B.; Schmuck, S. Sentinel-1 Mission Operations Concept. In Proceedings of the 2012 IEEE International Geoscience and Remote Sensing Symposium, Munich, Germany, 22–27 July 2012; p. 4.
47. Kšeňak, L.; Pukanská, K.; Bartoš, K.; Blišťan, P. Assessment of the Usability of SAR and Optical Satellite Data for Monitoring Spatio-Temporal Changes in Surface Water: Bodrog River Case Study. *Water* **2022**, *14*, 299. [[CrossRef](#)]
48. Tsyganskaya, V.; Martinis, S.; Marzahn, P.; Ludwig, R. Detection of Temporary Flooded Vegetation Using Sentinel-1 Time Series Data. *Remote Sens.* **2018**, *10*, 1286. [[CrossRef](#)]
49. Huang, M.; Jin, S. Rapid Flood Mapping and Evaluation with a Supervised Classifier and Change Detection in Shouguang Using Sentinel-1 SAR and Sentinel-2 Optical Data. *Remote Sens.* **2020**, *12*, 2073. [[CrossRef](#)]
50. Schlaffer, S.; Chini, M.; Dorigo, W.; Plank, S. Monitoring surface water dynamics in the Prairie Pothole Region of North Dakota using dual-polarised Sentinel-1 synthetic aperture radar (SAR) time series. *Hydrol. Earth Syst. Sci.* **2022**, *26*, 841–860. [[CrossRef](#)]
51. Anusha, N.; Bharathi, B. Flood detection and flood mapping using multi-temporal synthetic aperture radar and optical data. *Egypt. J. Remote Sens. Space Sci.* **2019**, *23*, 207–219. [[CrossRef](#)]
52. GoogleDevelopers. FAO GAUL: Global Administrative Unit Layers 2015, First-Level Administrative Units. 2022. Available online: https://developers.google.com/earth-engine/datasets/catalog/FAO_GAUL_2015_level1 (accessed on 8 March 2022).
53. GoogleDevelopers. JRC Global Surface Water Mapping Layers, v1.3. 2022. Available online: https://developers.google.com/earth-engine/datasets/catalog/JRC_GSW1_3_GlobalSurfaceWater (accessed on 8 March 2022).
54. GoogleDevelopers. WWF HydroSHEDS Void-Filled DEM, 3 Arc-Seconds. 2022. Available online: https://developers.google.com/earth-engine/datasets/catalog/WWF_HydroSHEDS_03VFDDEM (accessed on 8 March 2022).
55. Tavus, B.; Kocaman, S.; Gokceoglu, C. Flood damage assessment with Sentinel-1 and Sentinel-2 data after Sardoba dam break with GLCM features and Random Forest method. *Sci. Total Environ.* **2021**, *816*, 151585. [[CrossRef](#)]
56. Laur, H.; Bally, P.; Meadows, P.; Sanchez, J.; Schaettler, B.; Lopinto, E.; Esteban, D. Derivation of the Backscattering Coefficient σ_0 in ESA ERS SAR PRI Products. In *Sentinel-1 SAR; Calibration*, E.S., Ed.; ESA: Paris, France, 2004.
57. Pramanick, N.; Acharyya, R.; Mukherjee, S.; Mukherjee, S.; Pal, I.; Mitra, D.; Mukhopadhyay, A. SAR based flood risk analysis: A case study Kerala flood 2018. *Adv. Space Res.* **2021**, *69*, 1915–1929. [[CrossRef](#)]
58. Haralick, R.M.; Shanmugam, K.; Dinstein, I.H. Textural Features for Image Classification. *IEEE Trans. Syst. Man Cybern.* **1973**, *6*, 610–621. [[CrossRef](#)]
59. Amitrano, D.; Di Martino, G.; Iodice, A.; Riccio, D.; Ruello, G. Unsupervised Rapid Flood Mapping Using Sentinel-1 GRD SAR Images. *IEEE Trans. Geosci. Remote Sens.* **2018**, *56*, 3290–3299. [[CrossRef](#)]
60. Tulbure, M.G.; Broich, M.; Vincius, P.; Gaines, M.; Ju, J.; Stehman, S.V.; Pavelsky, T.; Masek, J.G.; Yin, S.; Mai, J.; et al. Can we detect more ephemeral floods with higher density harmonized Landsat Sentinel 2 data compared to Landsat 8 alone? *ISPRS J. Photogramm. Remote Sens.* **2022**, *185*, 232–246. [[CrossRef](#)]
61. NADMA. *Monthly Report of Disasters in Malaysia*; National Disaster Management Agency: Putrajaya, Malaysia, 2022; p. 1.
62. Landuyt, L.; Van Wesemael, A.; Schumann, G.J.-P.; Hostache, R.; Verhoest, N.E.C.; Van Coillie, F.M.B. Flood Mapping Based on Synthetic Aperture Radar: An Assessment of Established Approaches. *IEEE Trans. Geosci. Remote Sens.* **2018**, *57*, 722–739. [[CrossRef](#)]
63. Clinton, N. Otsu’s Method for Image Segmentation. 2017. Available online: <https://medium.com/google-earth/otsus-method-for-image-segmentation-f5c48f405e> (accessed on 14 June 2022).
64. Otsu, N. A Threshold Selection Method from Gray-Level Histograms. *IEEE Trans. Syst. Man Cybern.* **1979**, *SMC-9*, 62–66. [[CrossRef](#)]
65. Baillarin, S.J.; Meygret, A.; Dechoz, C.; Petrucci, B.; Lacherade, S.; Tremas, T.; Isola, C.; Martimort, P.; Spoto, F. Sentinel-2 Level 1 Products and Image Processing Performances. In Proceedings of the 2012 IEEE International Geoscience and Remote Sensing Symposium, Munich, Germany, 22–27 July 2012; p. 4.
66. GoogleDevelopers. Sentinel-2 MSI: MultiSpectral Instrument, Level-2A. 2022. Available online: https://developers.google.com/earth-engine/datasets/catalog/COPERNICUS_S2_SR (accessed on 19 April 2022).
67. Stephens, E.; Schumann, G.; Bates, P. Problems with binary pattern measures for flood model evaluation. *Hydrol. Process.* **2013**, *28*, 4928–4937. [[CrossRef](#)]
68. Mason, D.C.; Bevington, J.; Dance, S.; Revilla-Romero, B.; Smith, R.; Vetra-Carvalho, S.; Cloke, H. Improving Urban Flood Mapping by Merging Synthetic Aperture Radar-Derived Flood Footprints with Flood Hazard Maps. *Water* **2021**, *13*, 1577. [[CrossRef](#)]

69. ChePa, N.; Hashim, N.L.; Yusof, Y.; Hussain, A. Adaptive Emergency Evacuation Centre Management for Dynamic Relocation of Flood Victims using Firefly Algorithm. *J. Telecommun. Electron. Comput. Eng.* **2016**, *8*, 115–119.
70. Harries, T.; Penning-Rowsell, E. Victim pressure, institutional inertia and climate change adaptation: The case of flood risk. *Glob. Environ. Chang.* **2011**, *21*, 188–197. [[CrossRef](#)]
71. Da Silva, N.A.; Webber, B.G.M.; Matthews, A.J.; Feist, M.M.; Stein, T.H.M.; Holloway, C.E.; Abdullah, M.F.A.B. Validation of GPM IMERG Extreme Precipitation in the Maritime Continent by Station and Radar Data. *Earth Space Sci.* **2021**, *8*, e2021EA001738. [[CrossRef](#)]
72. Mayowa, O.O.; Pour, S.H.; Shahid, S.; Mohsenipour, M.; BIN Harun, S.; Heryansyah, A.; Ismail, T. Trends in rainfall and rainfall-related extremes in the east coast of peninsular Malaysia. *J. Earth Syst. Sci.* **2015**, *124*, 1609–1622. [[CrossRef](#)]
73. Hammim, R. Number of flood evacuees in Johor increasing. In *New Straits Times*; New Straits Times Press (Malaysia) Berhad (NSTP): Johor Bahru, Malaysia, 2022.
74. Bernama. *Johor Latest to be Hit by Floods, Number of Evacuees up Elsewhere*; Free Malaysia Today: Kuala Lumpur, Malaysia, 2022.
75. Liang, J.; Tan, M.L.; Hawcroft, M.; Catto, J.L.; Hodges, K.I.; Haywood, J.M. Monsoonal precipitation over Peninsular Malaysia in the CMIP6 Hormesis experiments: The role of model resolution. *Clim. Dyn.* **2021**, *58*, 2783–2805. [[CrossRef](#)]
76. Tan, M.L.; Ibrahim, A.L.; Cracknell, A.P.; Yusop, Z. Changes in precipitation extremes over the Kelantan River Basin, Malaysia. *Int. J. Clim.* **2016**, *37*, 3780–3797. [[CrossRef](#)]
77. Tarpanelli, A.; Mondini, A.C.; Camici, S. Effectiveness of Sentinel-1 and Sentinel-2 for Flood Detection Assessment in Europe. *Nat. Hazards Earth Syst. Sci.* **2022**, 1–24.
78. Rana, V.K.; Suryanarayana, T.M.V. Evaluation of SAR speckle filter technique for inundation mapping. *Remote Sens. Appl. Soc. Environ.* **2019**, *16*, 100271. [[CrossRef](#)]
79. Pekel, J.-F.; Cottam, A.; Gorelick, N.; Belward, A.S. High-resolution mapping of global surface water and its long-term changes. *Nature* **2016**, *540*, 418–422. [[CrossRef](#)] [[PubMed](#)]